Article

A Ternary Model for Particle Packing Optimization

Taher M. Abu-Lebdeh [1], Ransford Damptey [2], Liviu Marian Ungureanu [3] and Florian Ion Tiberiu Petrescu [3,*]

[1] Department of Civil, Architectural, and Environmental Engineering, North Carolina A&T State University, Greensboro, NC 27411, USA; taher@ncat.edu

[2] Joint School of Nanoscience and Nanoengineering, North Carolina A&T State University, Greensboro, NC 27411, USA; rdamptey@aggies.ncat.edu

[3] "Theory of Mechanisms and Robots" Department, Faculty of Industrial Engineering and Robotics, University Politehnica of Bucharest, Splaiul Independentei Street 313, 060042 Bucharest, Romania; ungureanu.liviu.marian@gmail.com

* Correspondence: fitpetrescu@gmail.com; Tel.: +40-7240-40348

Abstract: Powder packing in metal powders is an important aspect of additive manufacturing (otherwise known as 3-D printing), as it directly impacts the physical and mechanical properties of materials. Improving the packing density of powder directly impacts the microstructure of the finished 3D-printed part and ultimately enhances the surface finish. To obtain the most efficient packing of a given powder, different powder blends of that material must be mixed to minimize the number of voids, irrespective of the irregularities in the particle morphology and flowability, thereby increasing the density of the powder. To achieve this, a methodology for mixing powder must be developed, for each powder type, to obtain the maximum packing density. This paper presents a model that adequately predicts the volumetric fraction of the powder grades necessary for obtaining the maximum packing density for a given powder sample. The model factors in the disparity between theoretical assumptions and the experimental outcome by introducing a volume reduction factor. We outline the model development steps in this paper, testing it with a real-world powder system.

Keywords: composites; powder; packing density; nanostructured materials; ternary model; additive manufacturing; laser printing

1. Introduction

Powder packing is a very important aspect of additive manufacturing (3-D printing), as it directly impacts materials' physical and mechanical properties. Improving the packing density of powder directly impacts the microstructure of the finished 3D-printed product and the surface finish. The American Society for Testing and Materials (ASTM), a global standards organization, defines AM as a process of joining materials to make objects from 3D model data, usually layer upon layer.

Computer-Aided Design (CAD) and Computer-Aided Manufacturing are the two components of the additive manufacturing process that ensure that parts are fabricated in precise geometry. CAD involves incorporating software programs used for the precise design of the part that needs to be printed.

The printed parts are developed and produced by 3-D printing equipment. The design of the part to be additively manufactured is sent to the printer. These 3-D printers consist of a powder bed and a roller, which spreads powder continuously—the final product results from printing the three-dimensional object layer-by-layer via a bottom-up approach. There are a variety of applications of additive manufacturing, which include (but are not limited to) ceramics, composites, metals, polymers, and composite systems.

The efficient assembly of solid particles is an important issue in material science, particularly in the subcategories of ceramics, powder metallurgy, and concrete technology. In each case, optimizing the packing density is necessary, particularly when the application

requires the deposition of materials.Optimal powder packing density results in a good enough quality of the deposited material. It is important to know apriorihow this density will result from the deposition processes. Predicting the density of deposited materials is an important decision-making objective;its accuracy is necessary in the case of metallurgy and ceramic technology, at least because the density of packaging in concrete technology is much more difficult to achieve today [1–9].

The limited uniaxial tests of discrete particle size distribution (PSD) packaging are often modeled on discrete element methods. The ternary packaging of spheres with uniform or non-uniform PSD for several particles is examined in a three-dimensional system (3D). Such studies address the effect of particle size ratio and particle size fraction on mixtures' structural and micromechanical properties.

The study of packaging structure generally also includes porosity and coordination numbers. In contrast, the investigation of micromechanical properties includes the distribution of normal contact forces and the transmission of packaging stress. Such a small-scale investigation of the effect of the particle size ratio relative to the structure and mechanics of ternary packaging can highlight a link between the properties of the sample and the value of the parameter when reaching its critical value [10–19].

Ternary mixtures represent the simplest way to study polydisperse granular packaging. A careful examination of their properties can lead to particle systems composed of three fractions of particle size. The method is frequently used in various areas of industry (chemistry, pharmacy, metallurgy, etc.) [20–29]. In most situations, it is necessary to perform numerical tests of limited uniaxial compression of granular packaging. This standard laboratory testing procedure is necessary to measure the mechanical properties of granular materials [30–41].

The particle packing directly impacts the packing density, in that the better the packing, the higher the density. It is known that the higher the packing density of the powder, the better the properties will be [42].

Finer powders tend to provide smoother finishes. However, finer powders are expensive to produce. In addition, for mono-sized mixtures, a minimum packing density can be attained, which places a limit on the maximum density attainable for fine powders. For this reason, scientists have been interested in finding ways to increase powder-packing density over the years. Packing is not to be confused with compaction, where morphological changes are made to the particles [43]. There are two types of packing, namely ordered and random packing. Most of the packing is random, except when packing follows a rigid or greedy algorithm, where packing is entirely simulated. There are two types of random packing, namely random loose and random dense packing. Each of these different packing methods will lead to different density outcomes. We are interested in maximizing density, so random dense packing would be of particular interest.

As aforementioned, researchers have formulated many models to predict particle packing density. Some models are either too complicated to apply, only consider a few parameters in the analysis, or donot consider the wall effect and loosening effect. Other models cannot predict the packing efficiency of the particulate mixtures despite theirpractical importance. Others recognize the existence of geometrical particle interaction but donot consider this interaction between particle groups. Several models claim to produce the same output despite the effect of the particle mean sizes. Previous studies have shown that the individual suitability of the packing models varies depending on the mean sizes of the particles and the ratio of the mean size of the particles being packed. Additionally, most packing models assume that the particles are regularly shaped spheres, but very few have considered a shape factor.

In this paper, a discrete model is developed by modifying the Furnas model for micro and nano-size metal powders used for additive manufacturing. It describes the discrete particle size distribution for densest packing. The primary assumption of the proposed model is that each grade of the powder will pack to its maximum density in the volume available. It considers the particle size ratio, mean size, specific gravity, voids ratio, and the

initial densities. The model describes the effect of geometrical interaction between different size classes on the maximum packing density, thus considering the wall and loosening effects. Additionally, in powder metallurgy, the powders produced are sufficiently spherical and fit the assumption that the particles are spherical.

For this paper, a simple ternary model that estimates both the volume fractions of three powder samples with known diameters required to produce the maximum packing density for a mixture involving each sample and the maximum packing density possible is proposed. This model is particularly useful for additive manufacturing applications involving a powder bed, such as Selective Laser Melting (SLM) and Selective Laser Sintering (SLS). The packing model can be used to improve the density of the powder bed, which in turn leads to the production of denser additively manufactured parts. This research project responded to the Department of Energy's Kansas City National Security Campus (KCNSC) request. They were looking to mix Boron powder and Boron fillers to produce additively manufactured (3-Dprinted) parts. To test the viability of the model, several Boron powders—filler mixtures were prepared and paired up against the optimal volume fractions of each component predicted by the model. It was found that the model compared well with the experimental results and is well suited for industrial applications.

2. Materials and Methods

To achieve the densest packing for a material, different grades of powder are mixed. The working assumption for this work is that the smaller particles will fill in between the interstices of the larger particlesin the mixing process, reducing the number of voids and consequently improving the powder packing. By mixing different powder grades, larger particles can take the place of smaller particles, hence improving the denseness of the mixture (Figure 1) [44].
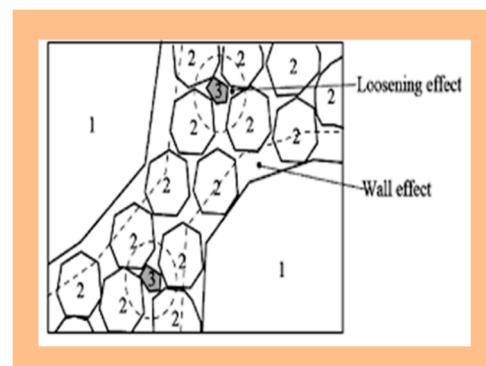

Figure 1. Wall and Loosening Effect [44].

These factors directly impact the packing density. In a coarse powder-dominant mixture, when fine particles are not small enough to fit into interstitial spaces, we term this the loosening effect. On the other hand, in cases where fine powder makes the bulk of the mixture, coarse particles may displace fine particles, but when they are not large enough to fill the spaces, they, in turn, create voids, and this phenomenon is termed wall effect. Wall and loosening effects tend to be more pronounced in mixtures where the diameters of each component of the binary mixture are similar (i.e., $\frac{d_1}{d_2} \to 1$).

The packing density of a powder sample is defined as a ratio of the solid volume to the total volume of the sample. The packing density is affected by the particle morphology (particle shape and size), the flowability of the powder, and particle size distribution.

Regardless of the size distribution, the random packing of spheres plays a significant role in various disciplines. Our interest is powder packing, and we may approximate the powder particles we use as spheres. The maximum packing that can be attainable for a unimodal mixture is 74%, as is the case in atomic packing. This is what makes binary and ternary mixtures of great interest in that the different sizes and weights will help

improve the packing density. These properties translate to micron-sized spheres, which is the size range of the powder particles of interest. The coordination number, being the average number of contacts a given sphere has in a powder sample, directly affects packing. In a mixture of multiple components, the coarse materials will tend to have a higher coordination number than the finer particles due to a higher surface area, which translates to more opportunities for the larger particles to be in contact with the smaller particles.

There have been many efforts to characterize powders used for additive manufacturing theoretically and quantitatively. The goal has been to predict the properties of the finished 3D-manufactured part and understand how adjusting specific parameters can impact the quality of the finished product (Figure 2) [45].
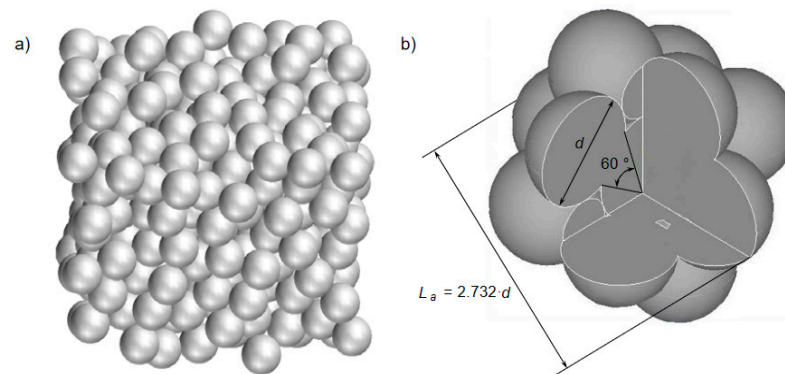

Figure 2. (**a**) Portion of a random packing of spherical particles (porosity = 30%); (**b**) Scheme of the sphere arrangement used to represent an agglomerate of spheres [45].

Researchers have formulated and studied many models to predict how packing density can be improved. During the sintering or melting process, the powder further undergoes changes. The challenge is to keep laser parameters as fixed as possible to ensure that a direct relationship is established between the packing density of the powder and the density of the printed part. (Figure 3) As such, methods that are invariant of laser parameters are often desired so that manufacturers can be assured that densely packed powder will yield dense AM parts. The models can be categorized into discrete models, design-of-experiment models, simulation models, and statistical modeling [46]. A schematic representation of particle interactions may be seen in Figure 4 [5–7].
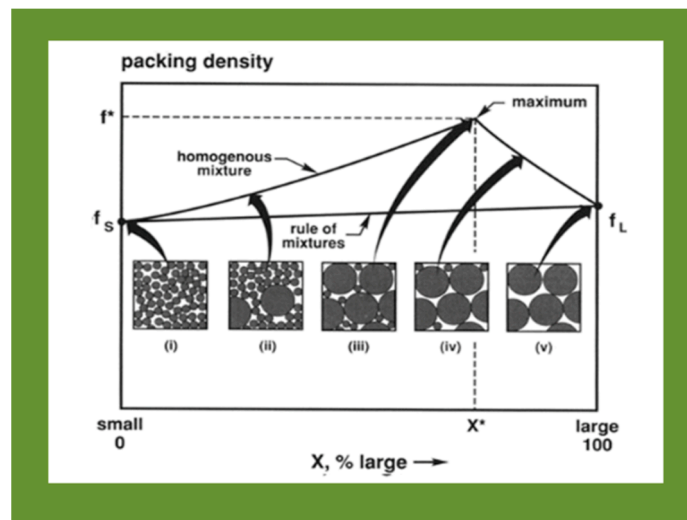

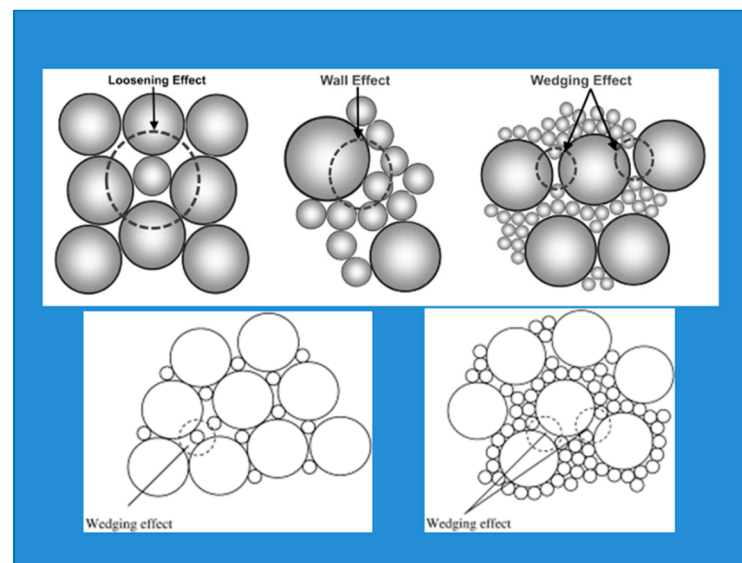**Figure 3.** Relationship between packing density and particle size [46].

Figure 4. Schematic representation of particle interactions [5–7].

Discrete models prove to be tailored to the specific powder ensemble, and as such, we would focus on those. Discrete models consist of binary mixture models, ternary mixture models, and multi-component mixture models based on the number of different samples that make up the mixture. Particle packing theory based on binary mixtures dates to the early 20th century, with C.C. Furnas being a pioneer inthis field. Furnas [47] based his model on a two-component bed of maximum density. For the purpose of this discussion, the larger particles will be referred to as coarse, and the smaller particles will be referred to as fine. He shows that to attain this maximum density of the bed, the absolute volume of the component with the larger particle size should be Z = 1/(1 + V), where V is the volume of voids in the packed bed. Other binary models include the Aim model [48], which factors in the wall effect in a packing vessel, the Toufar model, which describes the degree of packing, and the modified Toufar model [48], which modifies the value of the statistical factor. Some examples of the multi-component mixture models include Dewar, Stovall, and De Larrad models. The De Larrad models, comprising the Linear Packing Density Model (LPDM), Compressive Packing Model (CPM), and the Solid Suspension Model (SSM), a notable multi-component model system well suited for modeling multimodal mixtures. As efficient as the models are, none of them factor in a volume reduction factor that would affect the tap packing density of a powder bed and, ultimately, the density of the printed part.

The proposed model in this paper addresses the disparity between the theoretical packing density and the actual (experimental) packing density of a powder sample and proposes a way to calculate the volume [49–58].

3. Theory and Results

From a theoretical standpoint, packing smaller-sized spheres in the matrix of a mono-sized packing of particles increases the packing density, as the smaller ones fill the voids that existed before their introduction into the sphere matrix.

The addition of the smaller-sized particles improves the density as they fill the interstices between the large spheres, decreasing the number of voids in the packing and consequently increasing the packing density.

For instance, the highest packing density of a mono-sized sphere in an unbound space cannot be more than $\pi/(3\sqrt{2}) \approx 0.7404$, which means the solid material fills only 74% of the volume space.

Consider a container of unit volume with mono-sized spheres (s1) crushed into powder such that the powder occupies approximately 74% of the volume, and the air above is the remainder of the volume.

Let the solid volume be a $= \pi/(3\sqrt{2})$ so that the volume of voids is $(1 - a)$. One defines the void ratio, e, of component "i" as the ratio of the volume of voids (V_{vi}) to the bulk volume (i.e., V_i, the volume of the space that sample "i" occupies).

Assume that there are several particle sizes in a system, where the packing of a larger size leaves a certain fraction of voids. Each subsequent smaller size exactly fills the voids of the preceding size class without increasing the system's overall volume. Therefore, if infinitely small particles are successively introduced into the system in the manner described, the packing density could theoretically reach 100%. The packing mechanism in the proposed model is that the smaller particles are introduced into the interstices of the larger packed particles, reducing the voids in the system.

Furthermore, assume a stack of powder samples with decreasing sizes (average particle diameter) in a vertical container. Let r_i be the volume fraction of the coarser material of any two consecutive powder samples (1).

$$r_i = \frac{V_{si}}{V_{si} + V_{s(i+1)}} \tag{1}$$

Given the correlation between the void ratio and the volume fraction, we define a geometric series between any two consecutive particle size classes in terms of r_1 as follows (2):

$$r_1, 1 - r_1, (1 - r_1)\left(\frac{1 - r_2}{r_2}\right), (1 - r_1)\left(\frac{1 - r_2}{r_2}\right)\left(\frac{1 - r_3}{r_3}\right), \dots \tag{2}$$

A similar series can be defined for the weight fraction. The weight fraction of any powder sample, w_i, can be defined in terms of the specific true gravity of the sample. For the coarsest powder sample packed initially into our hypothetical vessel, we define $w_1 = G_1 v_{s1} = (1 - e_1)G_1$ where G_i is the specific gravity.

The percent composition of each powder component can then be defined in terms of the weight fractions. For the coarsest powder sample, that weight fraction is defined as $w_1 = G_1 v_{s1} = (1 - e_1)G_1$. Thus, the percent composition of the larger particles is given by (3):

$$\omega_1 = \frac{w_1}{w_1 + w_2} = \frac{(1 - e_1)G_1}{(1 - e_1)G_1 + e_1(1 - e_2)G_2} \tag{3}$$

As a note, the weight fraction, w_i, is not to be confused with the percent composition, ω_i. The apparent specific gravity, $G_a = (1 - e)G$, where G is the true specific gravity. Thus (4),

$$G_{a1} = (1 - e_1)G_1 \tag{4}$$

Upon simplification, we get the expressions for the volume fractions for a ternary system yielding the maximum packing density achievable as follows (5)–(7):

$$\frac{\omega_1}{G_{a1}} = \frac{1}{(1 - e_1)G_1 + e_1(1 - e_2)G_2} = v_1, \tag{5}$$

$$\frac{1 - \omega_1}{G_{a2}} = \frac{e_1}{(1 - e_1)G_1 + e_1(1 - e_2)G_2} = v_2 \tag{6}$$

$$\frac{(1 - \omega_1)\left(\frac{1 - \omega_2}{\omega_2}\right)}{G_{a3}} = \frac{e_1 e_2}{(1 - e_1)G_1 + e_1(1 - e_2)G_2} = v_3 \tag{7}$$

The bulk volume V_B, which is the sum of the above three expressions (5)–(7), becomes (8):

$$V_B = \frac{1 + e_1 + e_1 e_2}{(1 - e_1)G_1 + e_1(1 - e_2)G_2} \tag{8}$$

The equation above represents the total volume of a system made up of three different sizes and stacked upon another as separate layers. If the particles of the first component, d_1,

are relatively large, and all the other sizes (i.e., $d_2, d_3, \ldots$) are very small (ideally, infinitely small), then the voids created as a result of the d_1-sized particles will be exactly filled, and the final volume of the system will be the volume of the first component (largest sized particles).

Therefore, if each one of the smaller-sized particles exactly fills the voids created by the (larger) previously packed larger particle component, the total volume will just be v_1.

The reduction in volume resulting from filling the voids of component 1 with components 2 and 3 is equivalent to $(V - v_1)$. This will be the ideal case. However, for an actual system, the decrease in volume will be smallerthan the ideal case, as components 2 and 3 may not exactly fill the voids created by component 1. This decrease in volume is expressed as (9):

$$k_d(V_B - v_1) = k_d \left[\frac{e_1 + e_1 e_2}{(1 - e_1)G_1 + e_1(1 - e_2)G_2} \right] \tag{9}$$

k_d is a reduction factor ranging from 0 and 1 and can only be determined experimentally. Furnas experimented with different diameter ratios of different mixtures and, in each case, determined the corresponding contraction in volume that resulted [47]. With this data, he generated a quadratic fitting and an equation for the parameter y. It follows that thisparameter is exactly our parameter k_d. Below is a table of measured and calculated values for y and k_d. The measured values for y for corresponding $K^{1/n}$ values are from the paper by Furnas (see Table 1):

Table 1. Relationship between Reduction Factor and Contraction in Volume.

$K^{1/n}$	y_{obs}	$y_{computed}$	k_d
0	1	1	1
0.025	0.945	0.9355125	0.9355125
0.05	0.83	0.87305	0.87305
0.1	0.71	0.7542	0.7542
0.2	0.51	0.5408	0.5408
0.3	0.375	0.3598	0.3598
0.4	0.245	0.2112	0.2112
0.5	0.12	0.095	0.095
1	0	0	0

The expression for y in the Furnas model is given as (10):

$$y = 1 - 2.62k + 1.62k^2 \tag{10}$$

The graph below shows further how k_d and y are related (Figure 5):
Based on the relation between k_d and y, we define k_d similarly as (11):

$$k_d = y = 1 - 2.62k + 1.62 \tag{11}$$

where k is the ratio between consecutive sizes.

The total volume of the mixture then becomes (12):

$$V_f = V - k_d(V - v_1) = \frac{1 + e_1(1 + e_2)(1 - k_d)}{(1 - e_1)G_1 + e_1(1 - e_2)G_2} \tag{12}$$

The total weight (13),

$$w = \omega_1 + 1 - \omega_1 + (1 - \omega_1)\left(\frac{1 - \omega_2}{\omega_2}\right) = 1 + (1 - \omega_1)\left(\frac{1 - \omega_2}{\omega_2}\right) \tag{13}$$
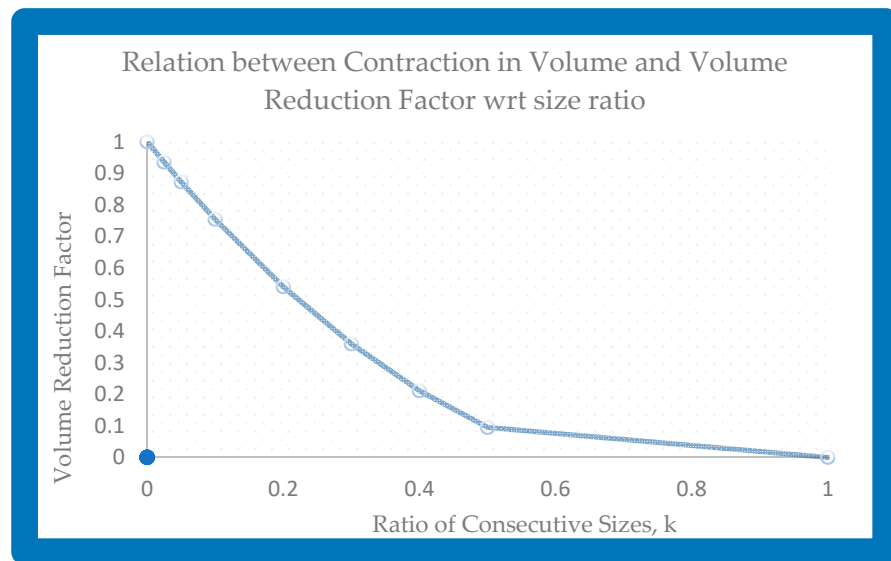
Figure 5. A graph of the volume reduction factor (vertical axis) vs. the ratio of consecutive sizes, k (horizontal axis).

The density, therefore, is calculated as (14):

$$\frac{(1-e_1)G_1 + e_1(1-e_2)G_2 + e_1e_2(1-e_3)G_3}{1 + e_1(1+e_2)(1-k_d)} \tag{14}$$

The solid volume (upon the incorporation of k_d) is (15):

$$V_s = \frac{1-e_1}{(1-e_1)G_1 + e_1(1-e_2)G_2} + \frac{e_1(1-e_2)(1-k_d)}{(1-e_1)G_1 + e_1(1-e_2)G_2} + \frac{(1-k_d)(1-e_3)e_1e_2}{(1-e_1)G_1 + e_1(1-e_2)G_2} \tag{15}$$

With this, and the bulk volume, we can determine the packing efficiency as (16):

$$\phi = \frac{V_s}{V_B} = \frac{1 - e_1 + e_1(1-e_2)(1-k_d) + e_1e_2(1-e_3)(1-k_d)}{1 + e_1(1+e_2)(1-k_d)} \tag{16}$$

This is the very general formula for a ternary mixture. In the theoretical scenario where each of the component powders in the mixture has the same void ratio (i.e., $e_1 = e_2 = e_3 = e$), the expression for packing density simplifies to $\phi = 1 - e$.

4. Discussion

Authors have tested the model with the Furnas model [47] for a three-component mixture to see if similar results were obtained for the maximum density, the volume of each component, and the percent fraction of each component that produces the maximum density.

The paper cited above includes an example problem where limestone, fine sand, and cement are mixed. The Furnas model is used to calculate the maximum density and the corresponding volume and volume fraction of each component. Void ratios (e_i), specific gravities (G_i), and average diameters of the components (d_i) were given as follows (see Table 2).

Table 2. Example Data for Calculation of Packing Density.

	Limestone	Fine Sand	Cement
d_i (in)	2	$\sqrt{2 \times 0.001} = 0.045$	0.001
e_i	0.48	0.42	0.52
G_i	2.5	2.65	3.10

To maintain the symmetric size distribution of the mixture, we find the average diameter of fine sand (d_2) as in the table above.

For this example problem, Furnas does not consider the volume contraction/reduction parameter in demonstrating the utility of his model, and as such, for comparison purposes, our k_d value will be kept as 0.

We use the expressions for density and volume from our model to directly compute the maximum density for this system, as well as determine the volume of each material that produces the maximum density after mixing (17):

$$
\begin{aligned}
\text{density} &= \frac{(1-e_1)G_1+e_1(1-e_2)G_2+e_1e_2(1-e_3)G_3}{1+e_1(1+e_2)(1-k_d)} \\
&= \frac{(1-0.48)(2.5)+(0.48)(1-0.42)(2.65)+(0.48)(0.42)(1-0.52)(3.10)}{1+(0.48)(1+0.42)(1-0)} = 1.39
\end{aligned}
\tag{17}
$$

Furnas calculated this value to be 1.39, which means our model estimates the value the Furnas model obtained within a 0.11% margin of error.

In obtaining the volume of each component, we use the expressions below (18):

$$
\begin{aligned}
\text{Volume for limestone, } v_1 &= \frac{1}{(1-e_1)G_1+e_1(1-e_2)G_2} = \frac{1}{(1-0.48)(2.5)+0.48(1-0.42)(2.65)} = 0.491 \\
\text{Volume for fine sand, } v_2 &= \frac{e_1(1-k_d)}{(1-e_1)G_1+e_1(1-e_2)G_2} = \frac{0.48(1-0)}{(1-0.48)(2.5)+0.48(1-0.42)(2.65)} = 0.236 \\
\text{Volume for cement, } v_3 &= \frac{e_1e_2(1-k_d)}{(1-e_1)G_1+e_1(1-e_2)G_2} = \frac{(0.48)(0.42)(1-0)}{(1-0.48)(2.5)+0.48(1-0.42)(2.65)} = 0.0989
\end{aligned}
\tag{18}
$$

These volumes computed with our model are quite closely related to the values obtained with Furnas' model, which respectively are 0.493, 0.234, and 0.0986. Our model gives us a total volume of 0.825 (V_f), compared with 0.8260 for the Furnas model [47]. The proportion by volume of each component required to produce the maximum density of the system compare as follows (Table 3):

Table 3. Furnas model vs. our model.

Proportions for Max. Density:		Proportions –> Furnas Model		% Error
limestone	v_1/V_f = 59.5%	limestone	v_1/V_f = 59.7%	0.37%
fine sand	v_2/V_f = 28.5%	fine sand	v_2/V_f = 28.3%	0.75%
cement	v_1/V_f = 12.0%	cement	v_1/V_f = 12%	0.43%

The above values reveal that our model almost exactly predicts the proportions by volume required to produce concrete of maximum density. In addition, our model can also be used in several other applications where different powder proportions are required to create a maximum density mixture. This model proves to be very powerful and yet simple in its versatility of application. The results suggest that for any powder sample, we can theoretically and experimentally determine the maximum packing density of powder for any application, notably 3-D printing. This flexibility of the model is very valuable for industrial purposes. Even though research suggests that a ternary mixture is the best to achieve the maximum density of a given powder type, the model can be used to derive expressions for any powder mixture with multiple components. In addition to powder mixtures of the same material, this model can be applied to mixtures with different components, as with the concrete example problem that was used above. Case Study: Consider the three different sizes of Boron powder shown in Table 4.

The three powders were mixed at different ratios, resultingin different densities. As shown in Table 5, the maximum density obtained experimentally confirms the findings of the proposed model.

Table 4. Experimental Results.

Name of Powder	Boron Powder (Coarse)	Boron Powder (Middle)	Boron Powder (Fine)
Diameter (d_n), μm	106	90	75
Bulk Volume (V_b), cm^3	10.68 ± 0.17	9.58 ± 0.17	9.14 ± 0.12
Tap Volume (V_s), cm^3	8.50 ± 0.14	7.80 ± 0.14	7.60 ± 0.14
Volume of void (V_v), cm^3	2.18 ± 0.18	1.78 ± 0.18	1.54 ± 0.18
Specific Gravity, S	2.34	2.34	2.34
Void ratio/void percentage (e)	0.20 ± 0.08	0.19 ± 0.10	0.17 ± 0.12

Table 5. Different Mix Ratios and their Densities.

	Method	Mix Ratios	Density (g/cm^3)
1	Proposed model	27.67: 5.67: 1	1.69 ± 0.11
2	Experimental 1	27.67: 5.67: 1	1.63 ± 0.04
3	Experimental 2	27.67: 1: 5.67	1.44
4	Experimental 3	1: 5.67: 27.67	1.26
5	Experimental 4	1: 27.67: 5.67	1.29
6	Experimental 5	5.67: 27.67: 1	1.26
7	Experimental 6	5.67: 1: 27.67	1.24
8	Experimental 7	11.44: 11.44: 11.44	1.27

5. Conclusions

The size composition of a powder mixture is a very important factor in determining the spreadability of the powder mixture and the density of the 3D-printed product.

To attain the most efficient packing of a powder, different sizes of that powder must be mixed so that it minimizes the voids by allowing the smaller particles to fill in between the interstices of the larger particles.

A model that predicts the volume fraction of each powder size becomes necessary to predict the maximum possible powder density.

In this research project, we have developed a simple model that predicts the volumetric fractions of powder mixture that can yield the highest powder density. The model accounts for the disparities between theoretical assumptions and practical outcomes, such as volume reduction. The model equations are based solely on void ratios and true specific gravity.

The proposed model is a discrete model which assumes that each class of particle will pack to its maximum density in the volume available.

Although the proposed model is used to model ternary mixtures, it can be extended to include multi-component Mixtures.

For generalization purposes, the model assumes that the particles being packed are perfect spheres and that the size ratio between successive sizes is constant for the entire system.

Although the model is derived for metal powder mixtures, it can be applied to mixtures of other systems such as asphalt concrete, paint, rubber, coal storage, etc.

The proposed model can be further verified by determining the actual powder bed packing density for further work. This may be achieved by building a small hollow cube (container). Only the container is melted during the SLM process, leaving the unfused powder inside the cube box. After the build, the powder inside the container will be weighed to determine the powder bed packing density.

The authors recommend extending the model to include ceramic powder because packing density significantly influences the shrinkage and density of ceramic during sintering and the properties of the final ceramic product. However, particle shape greatly

influences the packing density of ceramic particles, especially, when particles of several size classes are used. Thus, both the shape factor and convexity ratio should be considered in the analysis.

References

1. Fehling, E.; Schmidt, M.; Walraven, J.; Leutbercher, T.; Frohlich, S. *Ultra-High Performance Concrete UHPC Fundamentals, Design, Examples*, 1st ed.; Ernst Wilhelm: Berlin, Germany, 2014.
2. Kwan, A.K.H.; Fung, W.W.S. Packing density measurement and modeling of fine aggregate and mortar. *Cem. Concr. Comp.* **2009**, *31*, 349–357. [CrossRef]
3. Yu, R.; Spiesz, P.; Brouwers, H.J.H. Mix design and properties assessment of ultra-high performance fiber reinforced concrete (UHPFRC). *Cem. Concr. Res.* **2014**, *56*, 29–39. [CrossRef]
4. De Larrard, F.; Sedran, T. Optimization of ultra-high-performance concrete by the use of a packing model. *Cem. Concr. Res.* **1994**, *24*, 997–1009. [CrossRef]
5. Kwan, A.K.H.; Chan, K.W.; Wong, V. A 3-parameter particle packing model incorporating the wedging effect. *Powder Technol.* **2013**, *237*, 172–179. [CrossRef]
6. Chan, K.W.; Kwan, A.K.H. Evaluation of particle packing models by comparing with published test results. *Particuology* **2014**, *16*, 108–115. [CrossRef]
7. Wong, V.; Kwan, A.K.H. A 3-parameter model for packing density prediction of ternary mixes of spherical particles. *Powder Technol.* **2014**, *268*, 357–367. [CrossRef]
8. Li, L.G.; Kwan, A.K.H. the Packing density of concrete mix under dry and wet conditions. *Powder Technol.* **2014**, *253*, 514–521. [CrossRef]
9. *EN 1097–3*; Tests for Mechanical and Physical Properties of Aggregates. Determination of Loose Bulk Density and Voids. European Committee for Standardization: Brussels, Belgium, 1998.
10. McGeary, R.K. Mechanical Packing of Spherical Particles. *J. Am. Ceram. Soc.* **1961**, *44*, 513–523. [CrossRef]
11. Rassolusly, S.M.K. The packing density of 'perfect' binary mixtures. *Powder Technol.* **1999**, *103*, 145–150. [CrossRef]
12. Zou, R.P.; Bian, X.; Pinson, D.; Yang, R.Y.; Yu, A.B.; Zulli, P. Coordination Number of Ternary Mixtures of Spheres. *Part. Part. Syst. Charact.* **2003**, *20*, 335–341. [CrossRef]
13. Wiacek, J. Geometrical parameters of binary granular mixtures with size ratio and volume fraction: Experiments and DEM simulations. *Granul. Matter* **2016**, *18*, 42. [CrossRef]
14. Voivret, C.; Radjaï, F.; Delenne, J.Y.; El Youssoufi, M.S. Space-filling properties of polydisperse granularmedia. *Phys. Rev. E* **2007**, *76*, 021301. [CrossRef] [PubMed]
15. Wiacek, J.; Molenda, M. Microstructure and micromechanics of polydisperse granular materials: Effect of the shape of particle size distribution. *Powder Technol.* **2014**, *268*, 237–343. [CrossRef]
16. Sánchez, J.; Auvient, G.; Cambou, B.Ł. Coordination number and geometric anisotropy in binary sphere mixtures. In *Geomechanics from Micro to Macro, Proceedings of IS-Cambridge, Cambridge, UK, 1–3 September 2014*; CRC Press: Boca Raton, FL, USA, 2014; Volume 1.
17. Taha, H.; Nguyen, N.-S.; Marot, D.; Hijazi, A.; Abou-Saleh, K. Micro-scale investigation of the role of finer grains in the behavior of bidisperse granular materials. *Granul. Matter* **2019**, *21*, 28. [CrossRef]
18. Westman, A.E.R.; Hugill, H.R. The packing of particles. *J. Am. Ceram. Soc.* **1930**, *13*, 767–779. [CrossRef]
19. Petrescu, R.V.V.; Machin, A.; Fontanez, K.; Arango, J.C.; Marquez, F.M.; Petrescu, F.I.T. Hydrogen for aircraft power and propulsion. *Int. J. Hydrogen Energy* **2020**, *45*, 20740–20764. [CrossRef]
20. Stovall, T.; De Larrard, F.; Buil, M. Linear Packing Density Model of Grain Mixtures. *Powder Technol.* **1986**, *48*, 1–12. [CrossRef]
21. Yan, Y.; Zhang, L.; Luo, X.; Li, C.; Hu, F. A new method for calculating the primary porosity of unconsolidated sands based on packing texture: Application to modern beach sand. *Mar. Petrol. Geol.* **2018**, *98*, 384–396. [CrossRef]
22. Mirsayar, M.M.; Joneidi, V.A.; Petrescu, R.V.V.; Petrescu, F.I.T.; Berto, F. Extended MTSN criterion for fracture analysis of soda-lime glass. *Eng. Fract. Mech.* **2017**, *178*, 50–59. [CrossRef]

23. Mota, M.; Teixeira, J.A.; Yleshin, A. Image modeling of mixed granular porous media. *Fluid Part. Sep. J.* **1999**, *12*, 71–79.
24. Wiacek, J.; Molenda, M.; Stasiak, M. Effect of a number of granulometric fractions on structure and micromechanics of compressed granular packings. *Particuology* **2018**, *39*, 88–95. [CrossRef]
25. Yi, L.Y.; Dong, K.J.; Zou, R.P.; You, A.B. Coordination Number of the Packing of Ternary Mixtures of Spheres: DEM Simulations versus Measurements. *Ind. Eng. Chem. Res.* **2011**, *50*, 8773–8785. [CrossRef]
26. Martin, C.L.; Bouvard, D. Isostatic compaction of bimodal powder mixtures and composites. *Int. J. Mech. Sci.* **2004**, *46*, 907–927. [CrossRef]
27. Iddir, H.; Arastoopour, H.; Hrenya, C.M. Analysis of binary and ternary granular mixtures behavior using the kinetic theory approach. *Powder Technol.* **2005**, *151*, 117–125. [CrossRef]
28. Göncü, F.; Durán, O.; Luding, S. Constitutive relations for the isotropic deformation of frictionless packings of polydisperse spheres. *C. R. Mécanique* **2010**, *338*, 570–586. [CrossRef]
29. Gong, J.; Nie, Z.; Zhu, Y.; Liang, Z.; Wang, X. Exploring the effects of particle shape and content of fines on the shear behavior of sand-fines mixtures via the DEM. *Comput. Geotech.* **2019**, *106*, 161–176. [CrossRef]
30. Gu, X.Q.; Yang, J. Discrete element analysis of elastic properties of granular materials. *Granul. Matter* **2013**, *15*, 139–147. [CrossRef]
31. Cundall, P.A.; Strack, O.D. A discrete element model for granular assemblies. *Géotechnique* **1979**, *29*, 47–65. [CrossRef]
32. Thornton, C.; Cummins, S.J.; Cleary, P.W. An investigation of the comparative behavior of alternative contact force models during inelastic collisions. *Powder Technol.* **2013**, *233*, 30–46. [CrossRef]
33. Furnas, C.C. Grading Aggregates I-Mathematical Relations for Beds of Broken Solids of Maximum Density. *Ind. Eng. Chem.* **1931**, *23*, 1052–1058. [CrossRef]
34. Shire, T.; O'Sullivan, C.; Hanley, K. The influence of finer fraction and size ratio on the micro-scale properties of dense bimodal materials. In *Geomechanics from Micro to Macro*; CRC Press: London, UK, 2014; Volume 1, pp. 231–236.
35. Fei, K. Experimental study of the mechanical behavior of clay-aggregate mixtures. *Eng. Geol.* **2016**, *210*, 1–9. [CrossRef]
36. Bodman, G.B.; Constantin, G.K. Influence of Particle Size Distribution in Soil Compaction. *Hilgardia* **1965**, *36*, 567–591. [CrossRef]
37. Lade, P.V.; Yamamuro, J.A., Jr.; Liggio, C.D. Effects of fines content on void ratio, compressibility, and static liquefaction of silty sand. *Geomech. Eng.* **2009**, *1*, 1–15. [CrossRef]
38. Sun, Y.; Xiao, Y.; Hanif, K.F. Compressibility dependence on the grain size distribution and relative density in sands. *Sci. China Technol. Sci.* **2015**, *58*, 443–448. [CrossRef]
39. Taiebat, M.; Mautabaruka, P.; Pellenq, R.; Radjai, F. Effect of particle size polydispersity on 3D packings of spherical particles. *EPJ Web Conf.* **2017**, *140*, 02030. [CrossRef]
40. Minh, N.H.; Cheng, Y.P. On the contact force distributions of granular mixtures under 1D-compression. *Granul. Matter* **2016**, *18*, 18. [CrossRef]
41. Andrade, J.E.; Avila, C.F.; Hall, S.A.; Lenoir, N.; Viggiani, G. Multiscale modeling and characterization ofgranular matter: From grain kinematics to continuum mechanics. *J. Mech. Phys. Solids* **2011**, *59*, 237–250. [CrossRef]
42. Romagnoli, M.; Rivasi, M.R. Optimal size distribution to obtain the densest packing: A different approach. *J. Eur. Ceram. Soc.* **2007**, *27*, 1883–1887. [CrossRef]
43. Santomaso, A.; Lazzaro, P.; Canu, P. Powder flowability and density ratios: The impact of granules packing. *Chem. Eng. Sci.* **2003**, *58*, 2857–2874. [CrossRef]
44. De Larrard, F. *Concrete Mixture Proportioning: A Scientific Approach*; Taylor & Francis: New York, NY, USA, 1999. [CrossRef]
45. Bertei, A.; Nucci, B.; Nicolella, C. Effective Transport Properties in Random Packings of Spheres and Agglomerates. *Chem. Eng. Trans.* **2013**, *32*, 1531–1536. [CrossRef]
46. German, R.M. Prediction of sintered density for bimodal powder mixtures. *Metall. Trans. A* **1992**, *23*, 1455–1465. [CrossRef]
47. Aversa, R.; Petrescu, R.V.; Petrescu, F.I.T.; Perrotta, V.; Apicella, D.; Apicella, A. Biomechanically Tunable Nano-Silica/P-HEMA Structural Hydrogels for Bone Scaffolding. *Bioengineering* **2021**, *8*, 45. [CrossRef] [PubMed]
48. Goltermann, P.; Johansen, V.; Palbol, L. Packing of aggregates: An alternative tool to determine the optimal aggregate mix. *ACI Mater. J.* **1997**, *94*, 435–443.
49. Geldart, D.; Abdullah, E.C.; Verlinden, A. Characterization of dry powders. *Powder Technol.* **2009**, *190*, 70–74. [CrossRef]
50. Duan, Y.; Zhang, H.; Sfarra, S.; Avdelidis, N.P.; Loutas, T.H.; Sotiriadis, G.; Kostopoulos, V.; Fernandes, H.; Petrescu, F.I.; Ibarra-Castanedo, C.; et al. On the Use of Infrared Thermography and Acousto—Ultrasonics NDT Techniques for Ceramic-Coated Sandwich Structures. *Energies* **2019**, *12*, 2537. [CrossRef]
51. FIT Petrescu, RVV Petrescu, Nuclear hydrogen structure and dimensions. *Int. J. Hydrogen Energy* **2019**, *44*, 10833–10837. [CrossRef]
52. Fadiel, A.A.M.; Abu-Lebdeh, T. Mechanical Properties of Concrete Including Wood Shavings as Fine Aggregates. *Am. J. Eng. Appl. Sci.* **2021**, *14*, 478. [CrossRef]
53. Abu-Lebdeh, T.M.; Kalejaiye, O.A. Evaluation of Binary and Ternary Models in Powder Packing Density for Additive Manufacturing Applications. *Am. J. Eng. Appl. Sci.* **2021**, *14*, 314–322. [CrossRef]
54. Petrescu, F.I.T. Advanced Dynamics Processes Applied to an Articulated Robot. *Processes* **2022**, *10*, 640. [CrossRef]
55. Ungureanu, L.M.; Petrescu, F.I.T. Dynamics of Mechanisms with Superior Couplings. *Appl. Sci.* **2021**, *11*, 8207. [CrossRef]
56. Zeng, Z.; Shi, G.; Petrescu, F.I.T.; Ungureanu, L.M.; Li, Y. Micro-Nano Machining TiO2 Patterns without Residual Layer by Unconventional Imprinting. *Appl. Sci.* **2021**, *11*, 10097. [CrossRef]

57. Machín, A.; Fontánez, K.; Arango, J.C.; Ortiz, D.; De León, J.; Pinilla, S.; Nicolosi, V.; Petrescu, F.I.; Morant, C.; Márquez, F. One-Dimensional (1D) Nanostructured Materials for Energy Applications. *Materials* **2021**, *14*, 2609. [CrossRef] [PubMed]
58. Roudsari, S.S.; Ungureanu, L.M.; Soroushnia, S.; Abu-Lebdeh, T.; Petrescu, F.I.T. Optimization of Fiber-Reinforced Polymer Bars for Reinforced Concrete Column Using Nonlinear Finite Element Algorithms. *Algorithms* **2022**, *15*, 12. [CrossRef]